(DOI will not work until issue is live.) DOI: http://dx.doi.org/10.2138/am-2015-5274

U-Th baddeleyite geochronology and its significance to date the emplacement of silica undersaturated magmas

Revision 1

Wan N. Wu [a], Axel K. Schmitt [a,*], Lucia Pappalardo [b]

[a] Department of Earth, Planetary and Space Sciences, University of California, Los Angeles CA 90095, USA

[b] Istituto Nazionale di Geofisica e Vulcanologia, Sezione di Napoli, Osservatorio Vesuviano, Naples, Italy

*** corresponding author**

Always consult and cite the final, published document. See http://www.minsocam.org or GeoscienceWorld

Abstract

Baddeleyite is a frequently found accessory mineral in silica undersaturated lavas. Because it is typically enriched in uranium, while having low initial lead, baddeleyite has long been a prime target for U-Pb geochronology of mafic rocks. The difficulties in retrieving small baddeleyite grains from volcanic samples and the lack of a detailed understanding of baddeleyite occurrence, however, have limited baddeleyite chronology largely to coarse-grained mafic intrusive rocks. Here, the development of U-Th in-situ baddeleyite analysis using Secondary Ionization Mass Spectrometry (SIMS) is presented together with an assessment of baddeleyite occurrence in Quaternary silica-undersaturated lavas from Campi Flegrei (Naples, Italy). Samples studied comprise the pre- and post Campanian Ignimbrite (ca. 40 ka) lava domes of Cuma and Punta Marmolite, and Astroni and Accademia, respectively. The in-situ sample preparation required initial identification of baddeleyite crystals from sawed and polished rock billets using scanning electron microscope (SEM) backscatter imaging and energy dispersive X-ray analysis. U-Th baddeleyite isochron ages for intra-caldera Astroni and Accademia lava domes are $5.01\,^{+2.61}_{-2.55}$ ka (MSWD = 2.0; n = 17) and $4.36\,^{+1.13}_{-1.12}$ ka (MSWD = 2.9; n = 24), respectively. The ages for Punta Marmolite ($62.4\,^{+3.9}_{-3.8}$ ka; MSWD = 1.2; n = 11) and Cuma ($45.9\,^{+3.6}_{-3.5}$ ka; MSWD = 2.2; n = 11) predate the Campanian Ignimbrite. Rapid baddeleyite crystallization at the time of emplacement is supported by petrologic observations that >50% of the baddeleyite crystals documented in this study occur either in vesicles or in vesicle-rich regions of the host lavas whose textures developed over timescales of few years to few decades based on microlite crystal size distribution (CSD) analysis. Radiometric U-Th baddeleyite ages are mostly in agreement with previously determined K-Ar eruption ages, except for the Punta Marmolite lava dome whose U-Th baddeleyite age predates the K-Ar age by ca. 15 ka.

Always consult and cite the final, published document. See http://www.minsocam.org or GeoscienceWorld

Baddeleyite thus records eruptive emplacement with little evidence for significant pre-eruptive crystal residence, and has potential as an eruption chronometer for Quaternary silica-undersaturated volcanic rocks.

Keywords: GEOCHRONOLOGY: baddeleyite; RADIOGENIC ISOTOPES: uranium series; IGNEOUS PETROLOGY: trachyte; NEW TECHNIQUE: secondary ionization mass spectrometry

Introduction

The accessory mineral baddeleyite (ZrO_2) has long been recognized as an ideal chronometer for mafic and ultramafic rocks because it has an essentially infinite initial U-parent to Pb-daugher ratio (e.g., Heaman and LeCheminant 1993; Heaman 2009; Söderlund et al. 2013). Recent advances in high-spatial resolution methods (e.g., Chamberlain et al. 2010; Li et al. 2010; Schmitt et al. 2010; Ibanez-Mejia et al. 2014) have also enabled in-situ analysis of crystals too fine to be separated by conventional heavy mineral enrichment techniques (cf. Söderlund and Johansson 2002). Despite a surge in baddeleyite ages produced over the past decade (Söderlund et al. 2013), ambiguities remain about their geochronologic significance. This is in part because the chemical abrasion pre-treatment (Mattinson 2005), now the standard for zircon geochronology, appears to have little effect in enhancing concordance for baddeleyite, and consequently minor Pb-loss may go unrecognized (Rioux et al. 2010). Unlike zircon, baddeleyite's magmatic stability and diffusion properties have not been experimentally calibrated (cf. Cherniak and Watson 2003; Watson and Harrison 1983; Boehnke et al. 2013), and therefore comparison of high-precision U-Pb ages between coexisting zircon and baddeleyite (where available) is commonly used to constrain its age significance. In some instances,

Always consult and cite the final, published document. See http://www.minsocam.org or GeoscienceWorld

baddeleyite and zircon have yielded concordant ages (Svensen et al. 2012), but baddeleyite ages both younger and older than co-existing zircon have also been detected (e.g., Corfu et al. 2013; Sell et al. 2014; Janasi et al. 2011). Whereas inheritance is rare in baddeleyite, reflecting the tendency of baddeleyite to become obliterated under normal metamorphic or igneous conditions via reactions with silica-enriched fluids or melts to form zircon (Davidson and van Breemen 1988; Heaman and LeCheminant 1993; Söderlund et al. 2013), it has been proposed that baddeleyite predating zircon by ca. 200 ka may represent early crystallization in an evolving magma system (Sell et al. 2014), and therefore baddeleyite may not always directly date magmatic emplacement. Conflicting evidence has also emerged regarding the retention of U and Pb in baddeleyite during energetic events such as shock heating during impacts (Niihara et al. 2012; Moser et al. 2013).

Because of the fundamental geochronological importance of baddeleyite, it is key to better understand how baddeleyite ages relate to the crystallization and emplacement of mafic magmas. For this, we present here the development of U-Th baddeleyite geochronology via in-situ analysis using Secondary Ion Mass Spectrometry (SIMS) and provide the first high-temporal (at ca. 1000-year resolution) record for baddeleyite crystallization in silica-undersaturated magmas. We focus on four Pleistocene-Holocene silica-undersaturated lavas from the Campi Flegrei (Naples, Italy) caldera complex. These lavas are ideal to test the feasibility of U-Th baddeleyite geochronology because (1) they contain abundant (albeit fine-grained) baddeleyite, (2) their eruption ages are mostly well constrained by K-Ar sanidine dating, and (3) they cover an age range favorable for U-Th disequilibrium dating. The comparison between U-Th baddeleyite ages and known eruption ages allows us to refine the understanding of the baddeleyite chronometer in the context of magma transfer and emplacement timescales.

Always consult and cite the final, published document. See http://www.minsocam.org or GeoscienceWorld

Geologic background, ages, and mineralogy of Campi Flegrei lava domes

Campi Flegrei (aka Phlegrean Fields) is an active caldera complex in close proximity to the city of Naples, Italy (Fig. 1). The most voluminous caldera-forming events, which shaped the nested caldera structure of the complex (e.g., Fedele et al. 2008; De Vivo et al. 2010) include the Campanian Ignimbrite and the Neapolitan Yellow Tuff eruptions. The Campanian Ignimbrite is dated at 40.6 ± 0.1 ka (recalculated Ar-Ar sanidine age; De Vivo et al. 2001; age uncertainties are reported as 1σ throughout this paper) for the distal pyroclastic flow units and an overlapping age of 41.7 ± 0.9 ka (U-Th/He zircon; Gebauer et al. 2014) for the proximal Breccia Museo deposit. The Neapolitan Yellow Tuff erupted at 14.9 ± 0.2 ka (Ar-Ar feldspar; Deino et al. 2004) and produced the eponymous tuff deposits on which the city of Naples is largely constructed. The most recent eruption within the Campi Flegrei region formed the Monte Nuovo cinder cone in 1538 CE (Di Vito et al. 1987).

Located within the caldera and straddling its boundaries (Fig. 1) are several pre- and post-caldera trachytic lava domes for which the occurrence of baddeleyite has been previously documented (e.g., Melluso et al. 2012). The oldest of these are the Punta Marmolite and Cuma domes which erupted at 47.5 ± 2.0 ka (K-Ar groundmass; Rosi and Sbrana, 1987) and 42.2 ± 0.7 ka (K-Ar sanidine; Lirer, 2011), respectively, whereas post-caldera Astroni and Accademia domes were emplaced at 3.3 ± 0.4 ka and 3.8 ± 0.3 ka, respectively (K-Ar sanidine; Cassignol and Gillot, 1982). The Punta Marmolite dome is trachytic to phonotrachytic in composition (SiO_2 = 58.9 - 59.2 wt. %) with sanidine and sodalite as the major phenocryst phase (Melluso et al. 2012). Cuma dome consists of trachyphonolite (SiO_2 = 59.2 to 60.7 wt. %) and is the most

Always consult and cite the final, published document. See http://www.minsocam.org or GeoscienceWorld

alkaline among the samples studied here. It contains phenocrysts of sanidine, clinopyroxene, amphiboles, and olivine (Melluso et al. 2012). Astroni dome is trachytic in composition (SiO_2 = 57.8 - 58.5 wt. %; Tonarini et al. 2009) and dominated by alkali feldspar phenocrysts, clinopyroxene, and biotite (Isaia et al. 2003) Accademia dome compositionally classifies as latitic to trachytic with SiO_2 ranging from 58.5 to 59.8 wt. % (Melluso et al. 2012). Phenocrysts comprise predominantly plagioclase, clinopyroxene, phlogopite and sanidine.

Methods

Sample preparation

Rock samples from Astroni (AS), Accademia (ACC), Punta Marmolite (PM), and Cuma (CUMA) lavas were collected in hand-sized pieces. Initially, attempts were made to extract baddeleyite from crushed and sieved (<250 μm) ACC rock powders. Rock powder (~50 g) was immersed in test tubes filled with 100 ml methylene iodide liquid (density 3.3 g/cm^3) and the dense fraction was separated from the supernate after centrifuging and liquid-N_2 freezing of the test-tube bottom. Magnetic minerals were separated from the dense fraction using a hand-magnet. No baddeleyite was identified in the non-magnetic fraction by optical inspection. Another aliquot of the ACC rock powder (<250 μm) was sent to University of Lund, Sweden, for water-shaking table separation (Söderlund and Johansson, 2002). This also did not yield any useable baddeleyite separate (Söderlund, pers. comm.). With the failure of conventional separation techniques, presumably because baddeleyite crystals are exceedingly small (<20 μm) and intergrown with less dense minerals, the samples were prepared for in-situ analysis. For this, rock pieces were cut into approximately ~2.5 cm × 4 cm billets at ~0.5 cm thickness and hand-polished with aluminum-oxide abrasive and 1 μm aluminum oxide powder. Baddeleyite crystals

Always consult and cite the final, published document. See http://www.minsocam.org or GeoscienceWorld

were identified by imaging the polished surfaces using Leo 1430 VP and Tescan Vega-3 XMU scanning electron microscopes (SEM) at UCLA by scanning at 250× magnification in variable pressure mode (air pressure in sample chamber ~15 Pa) using a backscatter detector set to high contrast and low brightness to readily visualize high average atomic number (high-Z) phases (Fig. 2). An energy dispersive X-ray analyzer (EDAX) attached to the SEM was used in distinguishing baddeleyite from other Zr-bearing phases. When baddeleyite was identified, crystals were imaged at various magnifications (50×, 250× and 1000×) on the SEM (Supplementary Fig. 1) as well as on an optical petrographic microscope (50× and 100×, total magnification of camera and microscope). Areas of interest were then diamond drilled as disks ~3 mm in diameter which were placed on adhesive tape together with pre-polished Phalaborwa reference baddeleyite crystals. The assembly was cast in epoxy using a ~25.4 mm diameter Teflon ring. Cleaning and coating with a conductive Au-layer followed standard practice for SIMS U-Pb dating at UCLA (e.g., Schmitt et al. 2010). The thick billets (instead of regular thin sections where cracks and voids are inevitably impregnated with epoxy), and variable pressure mode imaging without conductive C-coating were essential sample preparation steps to mitigate C-contamination of the samples which is detrimental for U-Th SIMS analysis (see below).

Secondary ionization mass spectrometry (SIMS) analysis

In-situ U-series analysis of baddeleyite was performed on a CAMECA ims 1270 large magnet radius secondary ionization mass spectrometer (SIMS) at UCLA. A primary $^{16}O^-$ beam with an intensity of ~30 nA and total impact energy of 22.5 keV was focused to an ~30 µm × 20 µm diameter oval spot (Fig. 2). Positive secondary ions were extracted at an accelerating voltage of 10 kV with an energy bandpass of 50 eV and analyzed at mass resolution (M/ΔM) of 4800 in multi-collector mode. The contrast aperture was set for maximum transmission, whereas the field

Always consult and cite the final, published document. See http://www.minsocam.org or GeoscienceWorld

aperture was individually adjusted using the HfO^+ secondary ion image to only transmit ions from the baddeleyite into the mass spectrometer at a lateral resolution between ~5 and 20 µm. Due to the strong enrichment of U (and Th to a lesser, but still substantial degree) in baddeleyite, contribution of U and Th ions from the periphery of the sampled area is expected to be negligible. Secondary ions were simultaneously detected using three electron multipliers (EM) by incrementing the magnetic field through a total of 5 magnet stations (11 mass stations) with pre-defined magnet settling and integration times defining one analysis cycle. This magnet sequence was then repeated, generally for 30 cycles per analysis, unless the signal intensity dropped sharply due to exhaustion of the target baddeleyite. Besides the key masses $^{230}ThO^+$, $^{232}ThO^+$, and $^{238}UO^+$, mass stations (in amu) for singly charged ions corresponding to $^{90}Zr_2O_4^+$ (243.79) and $^{92}Zr^{90}ZrO_4^+$ (245.79) were analyzed to track the Zr emission from baddeleyite. A background mass station corresponding to mass 246.3 was included to record EM backgrounds that could affect the adjacent $^{230}ThO^+$ (246.028) peak due to tailing from the more abundant $^{232}ThO^+$ peak. Mass station 244.0381 corresponding to $^{232}ThC^+$ was analyzed to monitor the presence of carbon in the analyzed region, because elevated $^{232}ThC^+$ would indicate a contamination of the analysis spot with C. The presence of C is detrimental to $^{230}ThO^+$ analysis because with abundant oxygen and Th in the target baddeleyite it forms the cluster molecule $^{232}Th_2CO^{2+}$, which is an unresolvable interference on mass $^{230}ThO^+$ (Schmitt et al., 2006). For this reason, C contamination during sample preparation must be minimized and the sample cleaning procedure must be thorough. Twenty one analyses for which $^{230}ThO^+$ was overwhelmed by the C-bearing interference were discarded.

U-Th standard calibration

Always consult and cite the final, published document. See http://www.minsocam.org or GeoscienceWorld

Phalaborwa baddeleyite (2060 Ma; Heaman 2009) was used as a reference to calibrate the relative sensitivity factor (RSF) for Th and U, and as a check for the accuracy of (^{230}Th)/(^{238}U) determinations. Because Th and U abundances in Phalaborwa baddeleyite are variable (Schmitt et al. 2010), the RSF was determined from $^{208}Pb^{*}/^{206}Pb^{*}$ (* = radiogenic after correction for common Pb using $^{208}Pb/^{204}Pb = 38.34$ and $^{206}Pb/^{204}Pb = 18.86$ for Southern California anthropogenic Pb as a surface contaminant; Sañudo-Wilhelmy and Flegal, 1994) in the same sample volume where Th and U (as ThO^{+} and UO^{+}) were analyzed (Fig. 3; Reid et al. 1997). This procedures assumes concordance in the ^{232}Th and ^{238}U decays (a reasonable assumption for Phalaborwa; Heaman 2009), and it harnesses the fact that the Pb isotopic ratio is not measurably fractionated during SIMS analysis (Reid et al. 1997). Phalaborwa was determined to be in secular equilibrium within ~2% uncertainty which we adopt as an estimate for the external reproducibility of the U/Th RSF (Fig. 4). To monitor Th and U instrumental fractionation, Phalaborwa reference baddeleyite was also analyzed in replicate throughout each analytical session by bracketing unknown analyses on each sample mount. In several analysis sessions between March 2013 and August 2014, the U/Th RSF varied from 1.02 to 1.22.

We estimate the useful yield (number of ions of an isotopically pure ion species divided by the total number of atoms of that isotope consumed during the analysis) for $^{230}ThO^{+}$ (the precision-limiting isotope species) to be ~2% by using zircon as a proxy due to a lack of baddeleyite with known concentrations. For secular equilibrium baddeleyite, this estimate corresponds to total of ~0.005 counts/μm^3/ppm U.

SIMS data treatment

Always consult and cite the final, published document. See http://www.minsocam.org or GeoscienceWorld

Data reduction was performed using the in-house ZIPS software at UCLA developed by C. Coath, which applied a secondary intensity drift correction by extrapolating between adjacent measurement cycles. Uncertainties were propagated using the standard error of extrapolated intensity ratios, which closely agrees with the Poisson counting error derived from integration of the raw counts, and the uncertainties of the RSF calibration. Error-weighted linear regression of the data was performed using equations in Mahon (1996).

Crystal size distribution (CSD) analysis

Microlite crystallization is induced by decompression during magma ascent in a conduit (e.g., Geschwind and Rutherford 1995; Hammer and Rutherford 2002; Couch et al. 2003a; 2003b; Martel and Schmidt 2003; Hammer 2008; Brugger and Hammer 2010). Hence, microlite groundmass textures in volcanic rocks can reveal information on the duration of the near-surface decompression path of magmas (e.g., Hammer et al. 1999; 2000; Cashman and Blundy 2000; Rutherford and Gardner 2000; Martel et al. 2000; Mastrolorenzo and Pappalardo 2006; Resmini 2007; Salisbury et al. 2008; Blundy and Cashmann 2001; 2008; Pappalardo et al. 2014). Crystal size distributions (CSD, Marsh 1988; Cashman and Marsh 1988) define semi-logarithmic relationships between population density (number of microlites per unit volume) vs. crystal size (maximum length) with the slope equal to -1/(growth rate × residence time). Thus, if the growth rate is known, the time of microlite crystallization in the conduit can be computed.

Lava samples from the same domes used for U-Th baddeleyite analysis were imaged by high-resolution photomicrographs of single thin sections. Plagioclase microlites were identified and measured using the software ImageJ to quantify area, orientation, and length of major and minor axes of a best-fitted ellipse to individual microlite crystals. The smallest crystals measured

Always consult and cite the final, published document. See http://www.minsocam.org or GeoscienceWorld

here were approximately 0.05 mm in size. 2D data determined with ImageJ were converted to 3-D CSDs using the program CSDCorrections 1.37 (Higgins 2000; 2002; 2006). Additional constraints for rock fabric and crystal aspect ratio are necessary to generate accurate CSD data. In all samples studied here the rock fabric was massive and realistic crystal aspect ratios were calculated using the CSDslice software (Morgan and Jerram 2006).

Results

Baddeleyite occurrence

Two rock-billets were scanned for sample AS from Astroni dome, and a total of 32 baddeleyite grains were identified. Most of the identified baddeleyite grains range between ~8 to 15 µm in long dimension and only few grains up to ~25 µm exist which tend to be highly elongate. Over half of the baddeleyite grains are associated within vesicle-rich areas, the rest are either inclusions in other mineral phases or enclosed by matrix. In total, 205 baddeleyite grains were documented from five rock billets of sample ACC from the Accademia lava dome. Baddeleyite grains range from ~10 to 30 µm in long dimension, and variably comprise elongate, equant and irregular shapes. Vesicle-associated baddeleyite crystals amount to 50% with the remainder hosted in the groundmass or present as inclusions in major mineral phases. A total of 42 baddeleyite grains were documented from four rock billets of sample PM from Punta Marmolite lava dome. Their long dimensions vary between ~7 and 15 µm, and their variability in shape is equivalent to sample ACC. About 70% of baddeleyite crystals from sample PM are associated with vesicles and only 30% are matrix-hosted without nearby vesicles. Sample CUMA from Cuma lava dome yielded the fewest baddeleyite crystals. Only 17 baddeleyite

Always consult and cite the final, published document. See http://www.minsocam.org or GeoscienceWorld

crystals total could be identified after scanning six rock billets. CUMA baddeleyite crystals range from ~7 to 12 μm in long dimension. In contrast to the other samples from Campi Flegrei, the majority (~80%) of crystals are matrix-hosted, and only ~20% are associated with vesicles. About 50% of the baddeleyite grains from the CUMA sample have zircon rims based on the observation of a darker BSE signal compared to the BSE-bright baddeleyite interior. Among the baddeleyite crystals with zircon rims, none were associated with vesicles.

Other accessory minerals with high BSE intensity comparable to those of baddeleyite were also detected in Campi Flegrei lavas. Besides baddeleyite, zircon, zirconolite ($CaZrTi_2O_7$) and pyrochlore $(Na,Ca)_2Nb_2O_6(OH,F)$ have been tentatively identified based on semi-quantitative EDAX analysis. The typical grain sizes of these accessories are <15 μm, with the exception of zirconolite grains from sample CUMA, where grain sizes are as large as ~80 μm.

The average whole rock Zr abundances of Astroni, Accademia, Punta Marmolite and Cuma lavas are 336, 466, 579, and 1002 ppm, respectively (Melluso et al. 2012; Tonarini et al. 2009; Fig. 5). In a 2-D contour plot of Zr versus SiO_2 concentration compiling 892 whole rock analyses of lavas from Campi Flegrei (GEOROC; Sarbas and Nohl, 2008) Zr and SiO_2 abundances for baddeleyite-bearing lavas are generally mid-range and broadly similar to others for which it is unknown whether they contain baddeleyite or not, except for the high-Zr Cuma lavas (Fig. 5). Whole rock Zr abundances, however, do not correlate with the petrographically observed baddeleyite abundances. Sample CUMA, for example, has the highest Zr abundance, but the lowest baddeleyite yield. Potential explanations for this unexpected observation are discussed below.

Baddeleyite U-Th ages

Always consult and cite the final, published document. See http://www.minsocam.org or GeoscienceWorld

Twenty-four individual baddeleyite crystals from sample ACC of the Accademia lava dome were analyzed. Baddeleyite crystals in sample ACC also revealed remarkably high (^{238}U)/(^{232}Th) activities ranging from ~20 to 100 for most of the baddeleyites analyzed. All data plot to the far right of the equiline attesting to a strong ^{230}Th deficit and a young age of the crystals. The analyses yielded a U-Th regression slope of 0.039 ± 0.001 corresponding to an isochron age of $4.36^{+1.13}_{-1.12}$ ka with an MSWD value of 2.9 (Fig. 6).

From sample AS of the Astroni lava dome, 17 baddeleyite grains were successfully analyzed. Baddeleyites from this sample show the highest (^{238}U)/(^{232}Th) activities (~190) among the samples studied here and they display strong ^{230}Th deficits. The analyses define a U-Th slope of 0.045 ± 0.023 with a mean square of weighted deviates (MSWD) value of 2.0, which corresponds to a U-Th isochron age of $5.01^{+2.61}_{-2.55}$ ka (Fig. 6).

Although sample CUMA of the Cuma lava dome had the lowest baddeleyite abundance, 11 out of 17 baddeleyite crystals could be successfully targeted for U-Th analysis. Their (^{238}U)/(^{232}Th) activities range between ~2 and 50, broadly similar to those of sample PM. In contrast to the other samples, (^{238}U)/(^{232}Th) in baddeleyite of the Cuma lava appear bimodally distributed. Baddeleyite grains without zircon rims yielded low (^{238}U)/(^{232}Th) activities whereas the high (^{238}U)/(^{232}Th) activities correspond to baddeleyite grains with zircon rims, except for one grain that has low (^{238}U)/(^{232}Th) activity. The U-Th regression slope is 0.34 ± 0.02 with an MSWD value of 2.2 and the resulting U-Th age is $45.9^{+3.6}_{-3.5}$ ka (Fig. 6).

A total of eleven baddeleyite grains from sample PM of the Punta Marmolite lava dome was successfully analyzed. Their (^{238}U)/(^{232}Th) activities range between ~3 to 40, and are on average lower compared to ACC. The U-Th regression slope is 0.43 ± 0.02 with an MSWD

Always consult and cite the final, published document. See http://www.minsocam.org or GeoscienceWorld

value of 1.2 and a corresponding U-Th age of $62.4^{+3.9}_{-3.8}$ ka (Fig. 6). A synoptic timeline of major Campi Flegrei eruptions and the new U-Th baddeleyite ages for lava domes in comparison to their respective eruption ages is summarized in Figure 7.

Discussion

Zr-bearing accessory minerals in Campi Flegrei lava flows

Reports for Zr-rich accessory minerals in lava flows are scarce (e.g., de Hoog and van Bergen, 2000; Carlier and Lorand, 2003; Stockstill et al. 2003; Moore and DeBari 2012; Melluso et al. 2012; 2014), and it remains unclear if this is due to the small crystal size of these phases impeding easy identification, or if this reflects a rarity of lava flows carrying these accessories. Predicting the occurrence of Zr-bearing phases in mafic lavas based on whole rock compositions also appears to be difficult (e.g., de Hoog and van Bergen 2000). This is supported by the counterintuitive lack of correlation between Zr whole rock concentrations and the observed occurrence pattern of baddeleyite in Campi Flegrei samples: the highest Zr concentration from the Cuma lava dome corresponds to the lowest abundance of baddeleyite, whereas the lowest Zr concentration from the Accademia lava dome corresponds to the highest abundance of baddeleyite. In consequence, this implies that baddeleyite is not always the primary control on Zr abundance in Campi Flegrei volcanic rocks. For silica-saturated evolved rocks, in particular if they are plutonic (e.g., Gromet and Silver, 1983), it has been a long-standing notion that zircon is the dominant host for Zr, but the observations above illustrate that the sequestration of Zr in more mafic rocks is less well understood. Zr partitioning into major phases during basalt crystallization is generally negligible, with the exception of clinopyroxene (Cpx) which has the highest partitioning values for Zr (D_{Zr} between 0.27 and 1.01; Vannucci et al. 1998) compared to

Always consult and cite the final, published document. See http://www.minsocam.org or GeoscienceWorld

other minerals such as olivine, plagioclase, and Fe-Ti oxides where Zr is strongly incompatible. This implies that Zr in mafic lavas is either hosted by glass or groundmass (and some in Cpx), or in other accessory minerals. Zr abundances in interstitial glass or groundmass were not analyzed here, but the presence of other Zr-bearing accessory minerals was frequently observed during SEM scanning of rock billets. One explanation for the unexpected lack of correlation between whole rock Zr abundance and petrographically observed baddeleyite is therefore a competition between baddeleyite and other Zr-bearing accessory minerals. In the Cuma lava flow, which has a high whole rock Zr abundance but a low baddeleyite yield, such a Zr-bearing accessory mineral was identified as zirconolite. Zirconolite was frequently identified by EDAX while scanning for baddeleyites and the two EDAX spectra can be readily distinguished by the presence of Ca Kα and Ti Kα peaks in zirconolite which are absent in baddeleyite. Zirconolite grains in the CUMA sample are also often coarser than baddeleyite grains, ranging from 25 to 80 μm, and thus likely contribute strongly to the sample's high Zr concentration.

Baddeleyite U-Th age uncertainties

Although replicate analyses of Phalaborwa reference baddeleyite typically agree within analytical uncertainties, yielding MSWD values close to unity, the unknown baddeleyites sometimes show moderately elevated MSWD values. This suggests that U-Th baddeleyite ages are either affected by underestimation of analytical uncertainties and/or age dispersion that is not attributable to analytical bias. There are several confounding factors that could cause high MSWD values: (1) analytical uncertainties could have be underestimated, for example if analytical conditions vary between analysis of references and unknowns. This is a valid concern if C contamination is present. Although this is typically avoided during analysis of comparatively large reference baddeleyite grains, it is much less controllable in the in-situ analysis of

Always consult and cite the final, published document. See http://www.minsocam.org or GeoscienceWorld

baddeleyite where contamination from adjacent materials due to beam overlap and incomplete filtering by the field aperture is a concern (Fig. 2). Carbon contamination is monitored during the analysis on mass 244.03, but minor contributions from this interference may go undetected; (2) Compositional mismatch between reference baddeleyites and unknowns could cause bias that is not reflected in the error propagation. For example, if the analysis spot on a baddeleyite grain overlaps with mineral overgrowths of zirconolite or zircon, SIMS instrumental fractionation for U and Th is expected to differ from that calibrated for pure baddeleyite references. These so-called matrix-effects could lead to apparent age heterogeneities that are analytical artifacts due to inadequate calibration of the relative sensitivity factors for U and Th; (3) There is age heterogeneity in the unknown population. Because there is no other study that has determined baddeleyite crystallization time scales at the temporal resolution relevant to this study, it is presently premature to decide whether age heterogeneity in baddeleyite is common. In the light of these potential causes for the moderately elevated MSWD values in three of the samples, we expand all uncertainties by multiplying the errors with the square-root of the MSWD. The elevated MSWD reflects the scatter which is unaccounted for by propagating the known sources of uncertainty (i.e., counting statistics and Th/U RSF calibration). Although this procedure increases the U-Th baddeleyite age uncertainties by up to 70%, it does not significantly inhibit a meaningful comparison with known eruption ages.

Comparison to previously determined ages

The Astroni and Accademia lava domes from Campi Flegrei have been previously dated at 3.3 ± 0.4 ka and 3.8 ± 0.3 ka, respectively (K-Ar sanidine; Cassignol and Gillot, 1982). The baddeleyite U-Th ages of these two samples yielded $5.01\,^{+2.61}_{-2.55}$ ka and $4.36\,^{+1.13}_{-1.12}$ ka. Both populations have slightly elevated MSWD values compared to 95% confidence acceptance

Always consult and cite the final, published document. See http://www.minsocam.org or GeoscienceWorld

interval (Mahon, 1996). This indication of minor age heterogeneity in the sample, or an underestimation of analytical uncertainties, however, are accounted for by our error calculation. Thus, U-Th baddeleyite ages of Astroni and Accademia are in agreement with the previously determined ages within analytical uncertainties. Age uncertainties suggest that baddeleyite crystallization was comparatively rapid, within analytical resolution (~1,000 years in the case of sample ACC). Rapid baddeleyite crystallization is compatible with the textural observation that many baddeleyite crystals are associated with vesicles. High temperature fluids have been implicated in the transport of Zr (e.g., de Hoog and van Bergen, 2000), and therefore baddeleyite likely crystallized coeval with vesicles expanding as a consequence of eruptive decompression and degassing.

The Cuma dome was previously determined by K-Ar sanidine dating to have an eruption age of 42.2 ± 0.7 ka (Lirer, 2011) and the U-Th baddeleyite age reported here is $45.9\,^{+3.6}_{-3.5}$ ka, again with a minor overdispersion compared to propagated analytical errors. The K-Ar sanidine and U-Th baddeleyite ages are consistent with each other which indicates that baddeleyite in the Cuma lava crystallized within a short time period around the time of eruption.

An eruption age of 47.5 ± 2.0 ka for Punta Marmolite dome was previously determined by K-Ar groundmass dating (Rosi and Sbrana, 1987). The U-Th baddeleyite age reported here of $62.4\,^{+3.9}_{-3.8}$ ka is significantly older than the previously reported K-Ar age, but it shows no excess scatter beyond assigned analytical uncertainties. Both ages for the Punta Marmolite dome are consistent with field observations that ca. 40 ka Campanian Ignimbrite deposits overlie Punta Marmolite lavas in outcrop. It presently remains unresolved whether Punta Marmolite lavas erupted earlier than previously assumed based on K-Ar dating, or if there was a significant hiatus between baddeleyite crystallization and eruption. The uniformity of baddeleyite ages in Punta

Always consult and cite the final, published document. See http://www.minsocam.org or GeoscienceWorld

Marmolite lava, and the lack of protracted pre-eruptive baddeleyite crystallization in the Astroni, Accademia, and Cuma samples, however, suggest that a crystallization hiatus is an unlikely scenario. The comparison between U-Th baddeleyite and K-Ar ages also has limitations in that post-eruption disturbance of the K-Ar system is possible during subsequent phases of hydrothermal activity. Unfortunately, no other eruption age constraints for Punta Marmolite are available, which reflects the dearth of geochronological methods available to date young silica undersaturated lava flows.

Inferences on the crystallization time of the baddeleyite during magma decompression and degassing

Microlite groundmass textures constrain the timescales of magma decompression and degassing during the emplacement of the lava domes. All CSDs of the studied lavas display sublinear trends with gentle slopes ranging from -16 to -28 for the logarithm of population density vs. crystal size (Supplementary Fig. 2). Estimates of crystallization times are obtained from the calculated slopes if constant crystal growth rates can be assumed. For magmas that crystallize under comparatively small degrees of undercooling (evident by the lack of skeletal growth textures and consistent with the emplacement of comparatively massive dome laves) we adopt plagioclase growth rates of 10^{-9} to 10^{-10} mm s^{-1}; Cashman 1990; 1993). For these growth rates, plagioclase microlite CSD slopes for Campi Flegrei lavas translate into crystallization durations ranging from few years to few decades during magma decompression associated to dome expansion. Because baddeleyite crystallized late, as evident from its common association with vesicles, its crystallization duration is expected to be commensurate to the duration of microlite crystallization triggered by decompression. Radiometric dating evidence for formation

Always consult and cite the final, published document. See http://www.minsocam.org or GeoscienceWorld

of baddeleyite in a very short time period around the time of eruption is thus supported by brief timescales resulting from CSD analyses.

Significance of U-Th baddeleyite ages

Because little is known about baddeleyite stability in silica-undersaturated magmas, interpreting the significance of U-Th baddeleyite ages at present relies solely on the available petrographic and textural information, and the comparison with known eruption ages. It is clearly evident, however, that baddeleyite abundance cannot simply be predicted by whole rock Zr abundances relative to a differentiation index such as SiO_2 abundances (Fig. 5). Based on the observations made from the baddeleyite-bearing lava flows studied here, the majority of baddeleyite crystals occurs along vesicle walls or in vesicle fillings. This petrographic evidence implies late-stage crystallization of baddeleyite, and further supports the notion that U-Th baddeleyite ages approximate the eruption ages for their host lavas. Some baddeleyite crystals were documented to reside in the matrix and/or as inclusions in phenocrysts. In these cases, U-Th baddeleyite ages may reflect pre-eruptive crystallization, but in the samples studied no significant difference was detected between the ages for baddeleyite crystals that are present in vesicles and those in the matrix or phenocrysts.

Baddeleyite ages in terrestrial and extra-terrestrial mafic rocks are typically interpreted as magmatic ages, and thus can be distinguished from metamorphic or impact-related zircon formed at much later times (e.g., Söderlund et al. 2013; Moser et al. 2013). In rocks where magmatic baddeleyite and zircon crystals coexist, zircon often postdates baddeleyite (e.g., Sell et al. 2014). This has been interpreted as early crystallization of baddeleyite, which is then recycled as an

Always consult and cite the final, published document. See http://www.minsocam.org or GeoscienceWorld

antecryst (Miller et al. 2007) at a later stage when the magma has evolved to attain zircon saturation. For the volcanic samples studied here, however, there is no evidence for significant pre-eruptive crystallization of baddeleyite, except for the Punta Marmolite sample whose eruption age is presently only constrained by a vintage K-Ar groundmass date. The uniformity of most baddeleyite ages, and their textural association with vesicles in Campi Flegrei lavas implies that they mostly crystallized close to the eruption. Based on these results we tentatively conclude that antecrystic baddeleyite is rare, and that baddeleyite crystallizes close to emplacement or eruption. Baddeleyite chronometry is therefore applicable for dating the eruption of Quaternary mafic lavas, especially those that are too glassy, porous, altered or otherwise unsuitable for conventional dating techniques such as K-Ar or Ar-Ar.

Implications

This study is the first to successfully measure U-Th disequilibrium in baddeleyite crystals in Quaternary volcanic rocks. Among the approaches that were explored to prepare baddeleyite for SIMS analysis, in-situ analysis is currently deemed the only feasible sample preparation method. Although this involves labor-intensive scanning of many polished rock sections and subsequent mechanical separation of baddeleyite-bearing domains, this approach preserves the petrographic context of baddeleyite. In the studied samples here, U-Th baddeleyite ages were either equivalent to or older than the eruption ages determined by K-Ar (Ar-Ar) geochronology, and thus in accordance with baddeleyite being a magmatic mineral that cannot post-date the eruption. Based on petrographic observations that the majority of baddeleyite grains in the studied samples are located adjacent or within vesicles, it is concluded that baddeleyite

Always consult and cite the final, published document. See http://www.minsocam.org or GeoscienceWorld

crystallization is quasi coeval with shallow emplacement because vesicles are expected to nucleate and expand during eruptive decompression, either during ascent or eruption. CSD textural analysis indicates that these timescales are on the order of years to decades. Furthermore, comparisons between the U-Th baddeleyite ages from this study and previously reported K-Ar ages of the same samples mostly agree within uncertainties (the sample from Punta Marmolite dome being an exception). This establishes that U-Th baddeleyite geochronology is useful as an eruption chronometer for silica-undersaturated volcanic rocks <350 ka that lack other datable minerals (e.g., sanidine), or as a supplement to K-Ar (Ar-Ar) and ^{14}C dating methods. Baddeleyite has been discovered in volcanic rocks formed in a wide range of tectonic environments (e.g., the Cascade arc: Stockstill et al. 2003; Moore and DeBari 2012), but because it is often overlooked unless specifically targeted, little is known about how common it is. The full application range of U-Th baddeleyite geochronology, and the potential for dating other micro-crystals in Quaternary mafic rocks such as zirconolite, remains to be explored.

Acknowledgments

We thank journal editor Renat Almeev and reviewer Mary Reid for insightful comments. The field study in Campi Flegrei was supported by a National Geographic, Committee for Research and Exploration grant. National Science Foundation (NSF) Division of Earth Sciences (EAR) is acknowledged for grant 1250296. The ion microprobe facility at UCLA is partly supported by a grant from the NSF EAR Instrumentation and Facilities Program.

References

Blundy, J., and Cashman, K. (2001) Magma ascent and crystallization at Mount St. Helens, 1980-1986. Contributions to Mineralogy and Petrology, 140, 631-650.

Always consult and cite the final, published document. See http://www.minsocam.org or GeoscienceWorld

Blundy, J., and Cashman, K. (2008) Petrologic reconstruction of magmatic system variables and processes. Reviews in Mineralogy and Geochemistry, 69,179-239.

Boehnke, P., Watson, E.B., Trail, D., Harrison, T.M., and Schmitt, A. K. (2013) Zircon saturation re-revisited. Chemical Geology, 351, 324-334.

Brugger, C. R., and Hammer, J. (2010) Crystallization kinetics in continuous decompression experiments: Implications for interpreting natural magma ascent processes. Journal of Petrology 51, 1941-1965.

Carlier, G., and Lorand, J.P. (2003) Petrogenesis of a zirconolite-bearing Mediterranean-type lamproite from the Peruvian Altiplano (Andean Cordillera). Lithos, 69(1), 15-35.

Cashman, K.V., and Marsh, B.D. (1988) Crystal size distribution (CSD) in rocks and the kinetics and dynamics of crystallization II. Makaopuhi lava lake. Contributions to Mineralogy and Petrology, 99, 292-305.

Cashman, K., and Blundy, J. (2000) Degassing and crystallization of ascending andesite. Philosophical Transactions of the Royal Society of London. Series A: Mathematical, Physical and Engineering Sciences, 358, 1487- 1513.

Cashman, K.V. (1992) Groundmass crystallization of Mount St. Helens dacite, 1980-1986: A tool for interpreting shallow magmatic processes. Contributions to Mineralogy and Petrology, 109, 431-449.

Cashman, K.V. (1993) Relationship between plagioclase crystallization and cooling rate in basaltic melts. Contributions to Mineralogy and Petrology, 113, 126-142.

Always consult and cite the final, published document. See http://www.minsocam.org or GeoscienceWorld

Cassignol, C., and Gillot, P.Y. (1982) Range and effectiveness of unspiked potassium-argon dating: Experimental groundwork and applications. Numerical dating in stratigraphy, (Part 1), 159-179.

Chamberlain, K.R., Schmitt, A.K., Swapp, S.M., Harrison, T.M., Swoboda-Colberg, Nobert, Bleeker, Wouter, Peterson, T.D., Jefferson, C.W., and Khudoley, A.K. (2010) In situ U–Pb SIMS (IN-SIMS) micro-baddeleyite dating of mafic rocks: Method with examples. Precambrian Research, 183, 379-387.

Cherniak, D.J., and Watson, E.B. (2003) Diffusion in zircon. Reviews in Mineralogy and Geochemistry, 53, 113-143.

Corfu, F., Polteau, S., Planke, S., Faleide, J.I., Svensen, H., Zayoncheck, A., and Stolbov, N. (2013) U-Pb geochronology of Cretaceous magmatism on Svalbard and Franz Josef Land, Barents Sea Large Igneous Province. Geological Magazine, 150(06), 1127-1135.

Couch, S., Harford, C.L., Sparks, R.S.J., and Carroll, M.J. (2003a) Experimental constraints on the conditions of formation of highly calcic plagioclase microlites at the Soufriere Hills Volcano, Montserrat. Journal of Petrology, 44, 1455-1475.

Couch, S., Sparks, R.S.J., and Carroll, M.R. (2003b) The kinetics of degassing-induced crystallization at Soufriere Hills volcano, Montserrat. Journal of Petrology, 44, 1477-1502.

Davidson, A., and Van Breemen, O. (1988) Baddeleyite-zircon relationships in coronitic metagabbro, Grenville Province, Ontario: implications for geochronology. Contributions to Mineralogy and Petrology, 100, 291-299.

Always consult and cite the final, published document. See http://www.minsocam.org or GeoscienceWorld

de Hoog, J.C., and van Bergen, M.J. (2000) Volatile-induced transport of HFSE, REE, Th and U in arc magmas: evidence from zirconolite-bearing vesicles in potassic lavas of Lewotolo volcano (Indonesia). Contributions to Mineralogy and Petrology, 139(4), 485-502.

Deino, A.L., Orsi, G., De Vita, S., and Piochi, M. (2004) The age of the Neapolitan Yellow Tuff caldera-forming eruption (Campi Flegrei caldera – Italy) assessed by $^{40}Ar/^{39}Ar$ dating method. Journal of Volcanology and Geothermal Research, 133, 157–70.

De Vivo, B., Petrosino, P., Lima, A., Rolandi, G., and Belkin, H.E. (2010) Research progress in volcanology in the Neapolitan area, southern Italy: a review and some alternative views. Mineralogy and Petrology, 99, 1-28.

De Vivo, B., Rolandi, G., Gans, P.B., Calvert, A., Bohrson, W.A., Spera, F. J., and Belkin, H.E. (2001) New constraints on the pyroclastic eruptive history of the Campanian volcanic Plain (Italy). Mineralogy and Petrology, 73(1-3), 47-65.

Di Vito, M., Lirer, L., Mastrolorenzo, G., and Rolandi, G. (1987) The 1538 Monte Nuovo eruption (Campi Flegrei, Italy). Bulletin of Volcanology, 49, 608-615.

Fedele, L., Scarpati, C., Lanphere, M., Melluso, L., Morra, V., Perrotta, A., and Ricci, G. (2008) The Breccia Museo formation, Campi Flegrei, southern Italy: geochronology, chemostratigraphy and relationship with the Campanian Ignimbrite eruption. Bulletin of Volcanology 70, 1189-1219.

Gebauer, S.K., Schmitt, A.K., Pappalardo, L., Stockli, D.F., and Lovera, O.M. (2014) Crystallization and eruption ages of Breccia Museo (Campi Flegrei caldera, Italy) plutonic clasts

Always consult and cite the final, published document. See http://www.minsocam.org or GeoscienceWorld

and their relation to the Campanian ignimbrite. Contribution to Mineralogy and Petrology,167, 1-18.

Geschwind, C.H., and Rutherford, M.J. (1992) Cummingtonite and the evolution of the Mount St. Helens (Washington) magma system: An experimental study. Geology, 20, 1011-1014.

Gromet, L.P., and Silver, L.T. (1983) Rare earth element distributions among minerals in a granodiorite and their petrogenetic implications. Geochimica et Cosmochimica Acta, 47, 925-939.

Hammer, J.E. (2008) Experimental studies of the kinetics and energetic of magma crystallization. Reviews in Mineralogy and Geochemistry, 69, 9-59.

Hammer, J., and Rutherford, M. (2002) An experimental study of the kinetics of decompression-induced crystallization in silicic melt. Journal of Geophysical Research, 107(B1), ECV-8.

Hammer, J.E., Cashman, K.V., and Voight , B. (2000) Magmatic processes revealed by textural and compositional trends in Merapi dome lavas. Journal of Volcanology and Geothermal Research, 100, 165-192.

Hammer, J.E., Cashman, K.V., Hoblitt, R.P., and Newman, S. (1999) Degassing and microlite crystallization during pre-climactic events of the 1991 eruption of Mt. Pinatubo, Phillipines. Bulletin of Volcanology, 60, 355-380.

Heaman, L.M. (2009) The application of U–Pb geochronology to mafic, ultramafic and alkaline rocks: An evaluation of three mineral standards. Chemical Geology, 261, 43–52.

Heaman, L.M., and LeCheminant, A.N. (1993) Paragenesis and U-Pb systematcis of baddeleyite (ZrO_2). Chemical Geology, 110, 95-126.

Always consult and cite the final, published document. See http://www.minsocam.org or GeoscienceWorld

Higgins, M. D. (2000) Measurement of crystal size distributions. American Mineralogist, 85, 1105-1116.

Higgins, M. D. (2002) Closure in crystal size distributions (CSD), verification of CSD calculations, and the significance of CSD fans. American Mineralogist, 87, 171-175.

Higgins, M.D. (2006) Quantitative Textural Measurements in Igneous and Metamorphic Petrology. CambridgeUniversity Press, Cambridge, 276.

Ibanez-Mejia, M., Gehrels, G.E., Ruiz, J., Vervoort, J.D., Eddy, M.P., and Li, C. (2014) Small-volume baddeleyite (ZrO_2) U–Pb geochronology and Lu–Hf isotope geochemistry by LA-ICP-MS. Techniques and applications. Chemical Geology, 384, 149-167.

Isaia, R., D’Antonio, M., Dell’Erba, F., Di Vito, M., and Orsi, G. (2004) The Astroni volcano: the only example of closely spaced eruptions in the same vent area during the recent history of the Campi Flegrei caldera (Italy). Journal of Volcanology and Geothermal Research, 133, 171-192.

Janasi, V.D.A., de Freitas, V.A., and Heaman, L.H. (2011) The onset of flood basalt volcanism, Northern Paraná Basin, Brazil: A precise U-Pb baddeleyite/zircon age for a Chapecó-type dacite. Earth and Planetary Science Letters, 302(1), 147-153.

Li, Q.L., Li, X.H., Liu, Y., Tang, G.Q., Yang, J.H., and Zhu, W.G. (2010) Precise U–Pb and Pb–Pb dating of Phanerozoic baddeleyite by SIMS with oxygen flooding technique. Journal of Analytical Atomic Spectrometry, 25(7), 1107-1113.

Lirer L. (2011) I Campi Flegrei: storia di un campo vulcanico. Quaderni dell’Accademia Pontaniana, Naples, 1–180.

Always consult and cite the final, published document. See http://www.minsocam.org or GeoscienceWorld

Mahon, K.I. (1996) The New "York" regression: Application of an improved statistical method to geochemistry. International Geology Review, 38, 293-303.

Marsh, B.D. (1988) Crystal size distributions (CSD) in rocks and the kinetics and dynamics of crystallization I. Theory. Contributions to Mineralogy and Petrology, 99, 277-291.

Martel, C., and Schmidt, B. (2003) Decompression experiments as an insight into ascent rates of silicic magmas. Contributions to Mineralogy and Petrology, 144, 397–415.

Martel, C., Bourdier, J.L., Pichavant, M., and Traineau, H. (2000) Textures, water content and degassing of silicic andesites from recent plinian and dome-forming eruptions at Mount Pelee volcano (Martinique, Lesser Antilles arc). Journal of Volcanology and Geothermermal Research, 96, 191-206.

Mastrolorenzo, G., and Pappalardo, L. (2006) Magma degassing and crystallization processes during eruptions of high-risk Neapolitan volcanoes, Evidence of common equilibrium rising processes in alkaline magmas. Earth and Planetary Science Letters, 250, 164–181.

Mattinson, J.M. (2005) Zircon U–Pb chemical abrasion ("CA-TIMS") method: combined annealing and multi-step partial dissolution analysis for improved precision and accuracy of zircon ages. Chemical Geology, 220(1), 47-66.

Melluso, L., De'Gennaro, R., Fedele, L., Franciosi, L., and Morra, V. (2012) Evidence of crystallization in residual, Cl–F-rich, agpaitic, trachyphonolitic magmas and primitive Mg-rich basalt–trachyphonolite interaction in the lava domes of the Phlegrean Fields (Italy). Geological Magazine, 149, 532-550.

Always consult and cite the final, published document. See http://www.minsocam.org or GeoscienceWorld

Melluso, L., Morra, V., Guarino, V., de'Gennaro, R., Franciosi, L., and Grifa, C. (2014) The crystallization of shoshonitic to peralkaline trachyphonolitic magmas in a H_2O-Cl-F-rich environment at Ischia (Italy), with implications for the feeder system of the Campania Plain volcanoes. Lithos, 210-211, 242-259.

Miller, J.S., Matzel, J.E., Miller, C.F., Burgess, S.D., and Miller, R.B. (2007) Zircon growth and recycling during the assembly of large, composite arc plutons. Journal of Volcanology and Geothermal Research, 167(1), 282-299.

Moore, N.E., and DeBari, S.M. (2012) Mafic magmas from Mount Baker in the northern Cascade arc, Washington: probes into mantle and crustal processes. Contributions to Mineralogy and Petrology, 163(3), 521-546.

Morgan, D.J., and Jerram, D.A. (2006) On estimating crystal shape for crystal size distribution analysis. Journal of Volcanology and Geothermal Research, 154, 1-7.

Moser, D.E., Chamberlain, K.R., Tait, K.T., Schmitt, A.K., Darling, J.R., Barker, I.R., and Hyde, B.C. (2013) Solving the Martian meteorite age conundrum using micro-baddeleyite and launch-generated zircon. Nature, 499, 454-457.

Niihara, T., Kaiden, H., Misawa, K., Sekine, T., and Mikouchi, T. (2012) U-Pb isotopic systematics of shock-loaded and annealed baddeleyite: implications for crystallization ages of Martian meteorite shergottites. Earth and Planetary Science Letters, 341, 195-210.

Pappalardo, L., D'Auria, L., Cavallo, A., and Fiore, S. (2014) Petrological and seismic precursors of the paroxysmal phase of the last Vesuvius eruption on March 1944. Scientific Reports, 4.

Always consult and cite the final, published document. See http://www.minsocam.org or GeoscienceWorld

Reid, M.R., Coath, C.D., Harrison, T.M., and McKeegan, K.D. (1997) Prolonged residence times for the youngest rhyolites associated with Long Valley Caldera: ^{230}Th-^{238}U ion microprobe dating of young zircons. Earth and Planetary Science Letters, 150, 27-39.

Resmini, R.G. (2007) Modeling of crystal size distributions (CSDs) in sills. Journal of Volcanology and Geothermal Research, 161, 118-130.

Rioux, M., Bowring, S., Dudás, F., and Hanson, R. (2010) Characterizing the U–Pb systematics of baddeleyite through chemical abrasion: application of multi-step digestion methods to baddeleyite geochronology. Contributions to Mineralogy and Petrology, 160(5), 777-801.

Rosi, M., and Sbrana, A. (1987) Phlegraean fields. Quaderni de la Ricerca Scientifica. Consiglio nazionale delle ricerche., Roma, 114, 114-175.

Rutherford, M. J., and Gardner, J. E. (2000) Rates of magma ascent. In: Sigurdsson, H. S. (ed.) Encyclopedia of Volcanoes. San Diego, CA: Academic Press, 207-218.

Salisbury, M.J., Bohrson, W.A., Clynne, M., Ramos, F.C. and Hoskin, P. (2008) Multiple plagioclase crystal populations identified by crystal size distribution and in situ chemical data: Implications for timescales of magma chamber processes associated with the 1915 eruption of Lassen Peak, CA. Journal of Petrology, 49, 1755–1780.

Sañudo-Wilhelmy, S.A., and Flegal, A.R. (1994) Temporal variations in lead concentrations and isotopic composition in the Southern California Bight. Geochimica et Cosmochimica Acta, 58(15), 3315-3320.

Sarbas, B., and Nohl, U. (2008) The GEOROC database as part of a growing geoinformatics network. Geoinformatics.

Always consult and cite the final, published document. See http://www.minsocam.org or GeoscienceWorld

Schmitt, A.K., Chamberlain, K.R., Swapp, S.M., and Harrison, T.M. (2010) In situ U–Pb dating of micro-baddeleyite by secondary ion mass spectrometry. Chemical Geology, 269, 386-395.

Schmitt, A.K., Stockli, D.F., and Hausback, B.P. (2006) Eruption and magma crystallization ages of Las Tres Vírgenes (Baja California) constrained by combined ^{230}Th/^{238}U and (U–Th)/He dating of zircon. Journal of Volcanology and Geothermal Research, 158, 281-295.

Sell, B., Ovtcharova, M., Guex, J., Bartolini, A., Jourdan, F., Spangenberg, J.E., Vicente, J.-C., and Schaltegger, U. (2014) Evaluating the temporal link between the Karoo LIP and climatic-biologic events of the Toarcian Stage with high-precision U–Pb geochronology. Earth and Planetary Science Letters, 408, 48-56.

Söderlund, U., and Johansson, L. (2002) A simple way to extract baddeleyite (ZrO2). Geochemistry Geophysics Geosystems 3.

Söderlund, U., Ibanez-Mejia, M., El Bahat, A., Ernst, R.E., Ikenne, M., Soulaimani, A., Youbi, N., Cousens, B., El Janati, M., and Hafid, A. (2013) Reply to Comment on “U–Pb baddeleyite ages and geochemistry of dolerite dykes in the Bas-Drâa inlier of the Anti-Atlas of Morocco: Newly identified 1380 Ma event in the West African Craton” by André Michard and Dominique Gasquet. Lithos, 174, 101-108.

Stockstill, K.R., Vogel, T.A., and Sisson, T.W. (2003) Origin and emplacement of the andesite of Burroughs Mountain, a zoned, large-volume lava flow at Mount Rainier, Washington, USA. Journal of volcanology and geothermal research, 119(1), 275-296.

Svensen, H., Corfu, F., Polteau, S., Hammer, Ø., and Planke, S. (2012) Rapid magma emplacement in the Karoo large igneous province. Earth and Planetary Science Letters, 325, 1-9.

Always consult and cite the final, published document. See http://www.minsocam.org or GeoscienceWorld

Tonarini, S., D'Antonio, M., Di Vito, M.A., Orsi, G., and Carandente, A. (2009) Geochemical and B–Sr–Nd isotopic evidence for mingling and mixing processes in the magmatic system that fed the Astroni volcano (4.1–3.8 ka) within the Campi Flegrei caldera (southern Italy). Lithos, 107, 135-151.

Vannucci, R., Bottazzi, P., Wulff-Pedersen, E., and Neumann, E.R. (1998) Partitioning of REE, Y, Sr, Zr and Ti between clinopyroxene and silicate melts in the mantle under La Palma (Canary Islands): implications for the nature of the metasomatic agents. Earth and Planetary Science Letters, 158, 39-51.

Wang, Y., Hsu, W., Guan, Y., Li, X., Li, Q., Liu, Y., and Tang, G. (2012) Petrogenesis of the Northwest Africa 4734 basaltic lunar meteorite. Geochimica et Cosmochimica Acta, 92, 329-344.

Watson, E.B., and Harrison, T.M. (1983) Zircon saturation revisited: temperature and composition effects in a variety of crustal magma types. Earth and Planetary Science Letters, 64, 295-304.

Figure Captions

Figure 1. Simplified geologic map of Campi Flegrei caldera showing sampling locations.

Figure 2. Backscatter images of baddeleyite grains before and after SIMS analysis; (a) and (b) Accademia dome; (c) and (d) Punta Marmolite dome; (e) and (f) Cuma dome; note the zircon rim around baddeleyite mantle in (e); (g) and (h) Astroni dome. Although overlap of the primary beam (dashed line in b, d, f, and h) with adjacent materials occurs, the effects of ion emission from the crater periphery are mitigated, albeit not completely eliminated especially in the case of C-bearing interferences, by inserting a square aperture (“field aperture”) into the secondary ion path.

Always consult and cite the final, published document. See http://www.minsocam.org or GeoscienceWorld

Figure 3. Phalaborwa baddeleyite reference $^{232}ThO^+/^{238}UO^+$ vs. $^{208}Pb^*/^{206}Pb^*$ (* = radiogenic after ^{204}Pb-based common Pb correction assuming $^{208}Pb/^{204}Pb$ = 38.34 and $^{206}Pb/^{204}Pb$ = 18.86 for anthropogenic Pb from Southern California; Sañudo-Wilhelmy and Felgal, 1994). Slope of regression corresponds to a relative sensitivity factor (RSF = measured U/Th divided by true U/Th) for baddeleyite analysis of 1.181 in this particular session.

Figure 4. U-Th isochron plot for Phalaborwa baddeleyite reference. Activities are indicated by parentheses. Data uncorrected for relative sensitivity (open circles), and corrected for relative sensitivity (black circles), are shown together with the equiline corresponding to (^{230}Th)/(^{238}U) = 1. After correction, the data define a slope that is indistinguishable from unity, indicating secular equilibrium for Phalaborwa baddeleyite.

Figure 5. Zr vs. SiO_2 for Campi Flegrei lavas. Symbols show the lava flows studied here, and colored fields the two-dimensional (2-D) relative probabilities for 892 rock compositions from the GEOROC database (http://georoc.mpch-mainz.gwdg.de) searched by location name = Campi Flegrei (Phlegraean Fields). Alternating solid and dashed lines indicate relative probabilities corresponding to the percentages of data points contained within each field.

Figure 6. U-Th baddeleyite isochron plot. (a) Accademia dome; (b) Astroni dome; (c) Cuma dome; (d) Punta Marmolite dome.

Figure 7. Schematic timeline of the major eruptive events of Campi Flegrei showing literature data together with U-Th baddeleyite ages from this study.

Supplementary Information

Always consult and cite the final, published document. See http://www.minsocam.org or GeoscienceWorld

Supplementary Table 1. U-Th baddeleyite results for Campi Flegrei lavas and Phalabowa reference.

Supplementary Figure 1. Backscatter electron images of baddeleyite from Campi Flegrei lavas analyzed for U-Th isotopic compositions.

Supplementary Figure 2. Crystal Size Distributions plot from Campi Flegrei lava domes.

Always consult and cite the final, published document. See http://www.minsocam.org or GeoscienceWorld

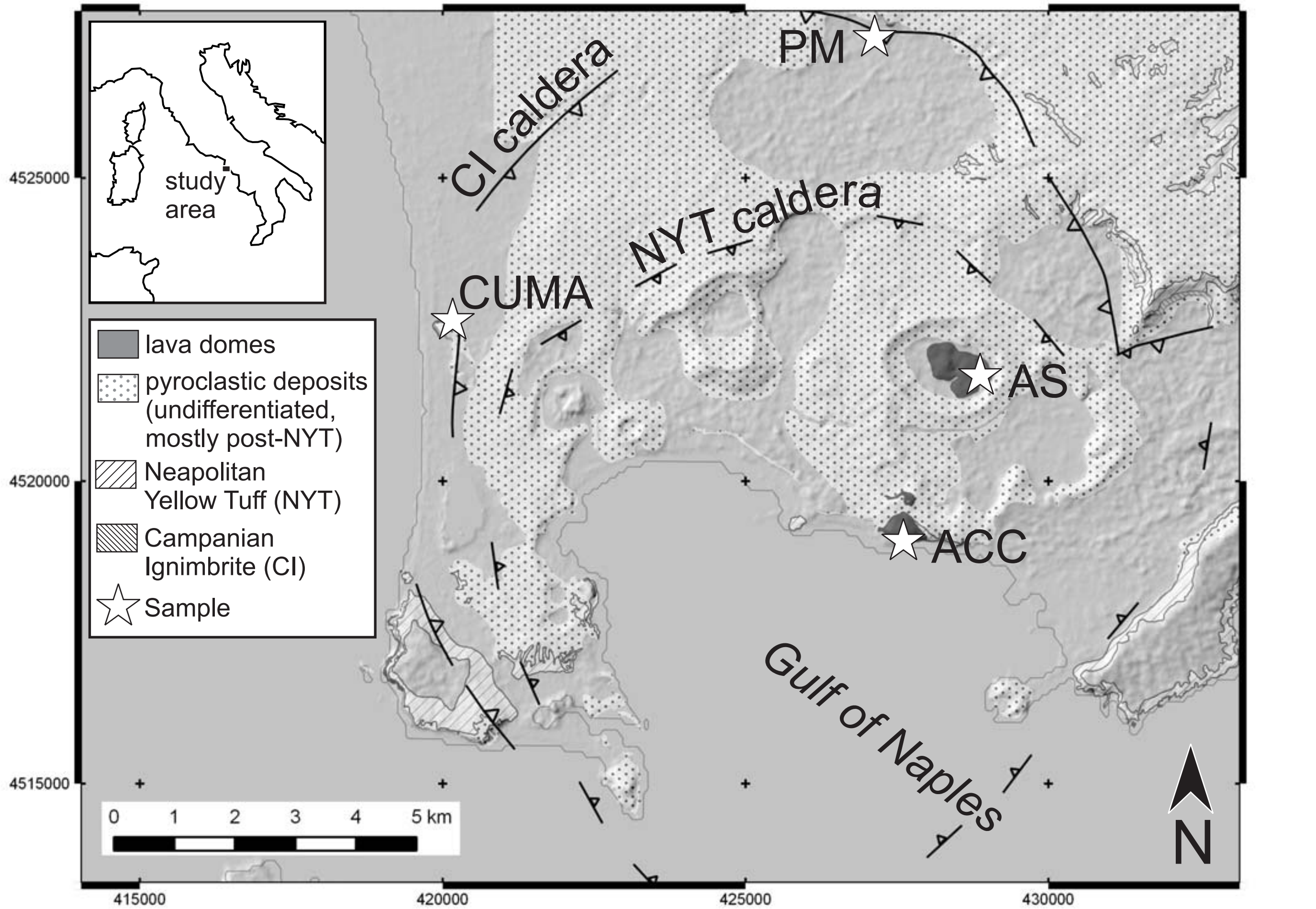

PM
CI caldera
NYT caldera
CUMA
AS
ACC
Gulf of Naples
study
area
lava domes
pyroclastic deposits
(undifferentiated,
mostly post-NYT)
Neapolitan
Yellow Tuff (NYT)
Campanian
Ignimbrite (CI)
Sample
0
1
2
3
4
5 km
N
4525000
4520000
4515000
415000
420000
425000
430000

Fig. 1: Wu et al.

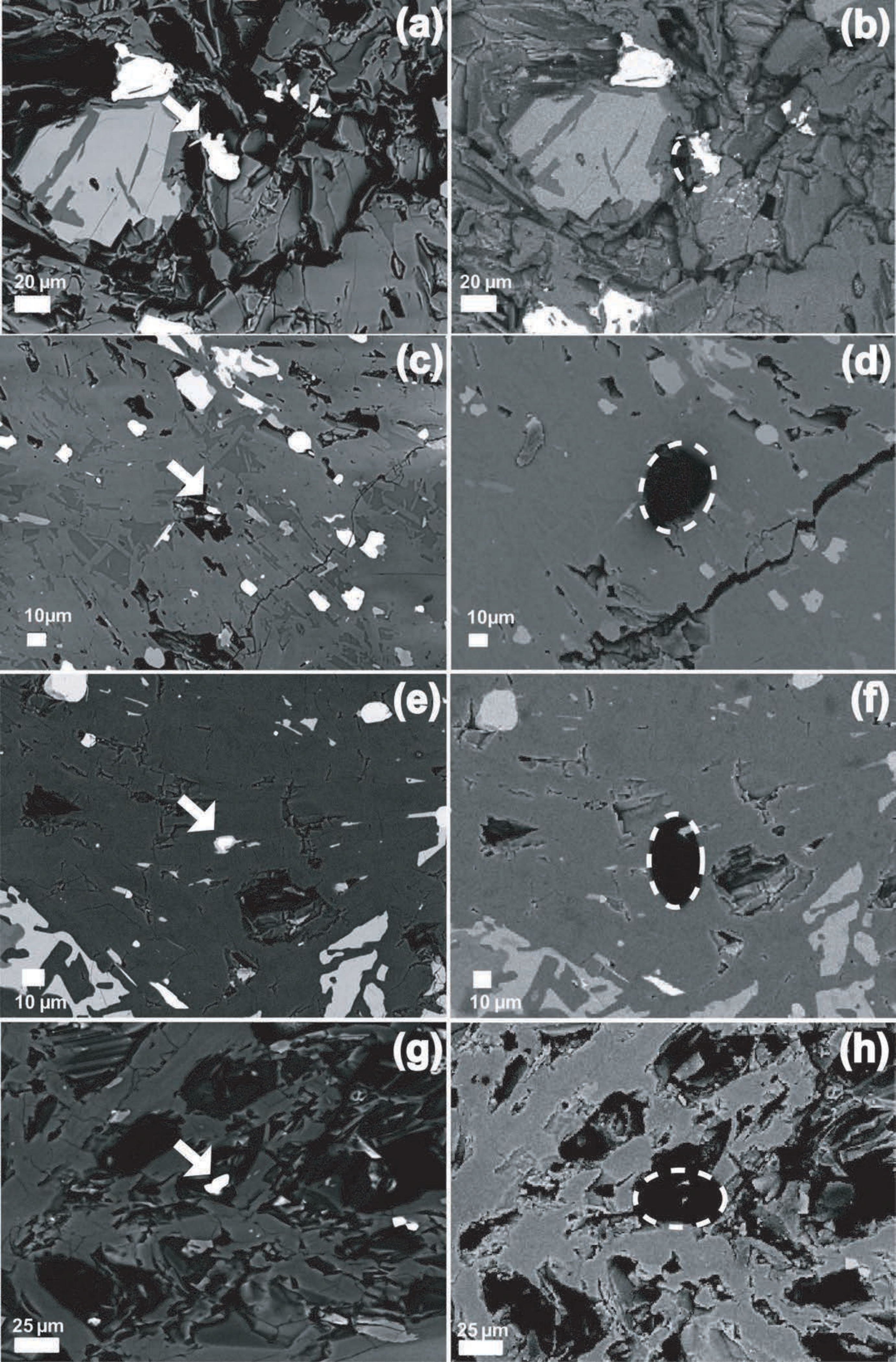
(a)
20 µm
(b)
20 µm
(c)
10µm
(d)
10µm
(e)
10 µm
(f)
10 µm
(g)
25 µm
(h)
25 µm

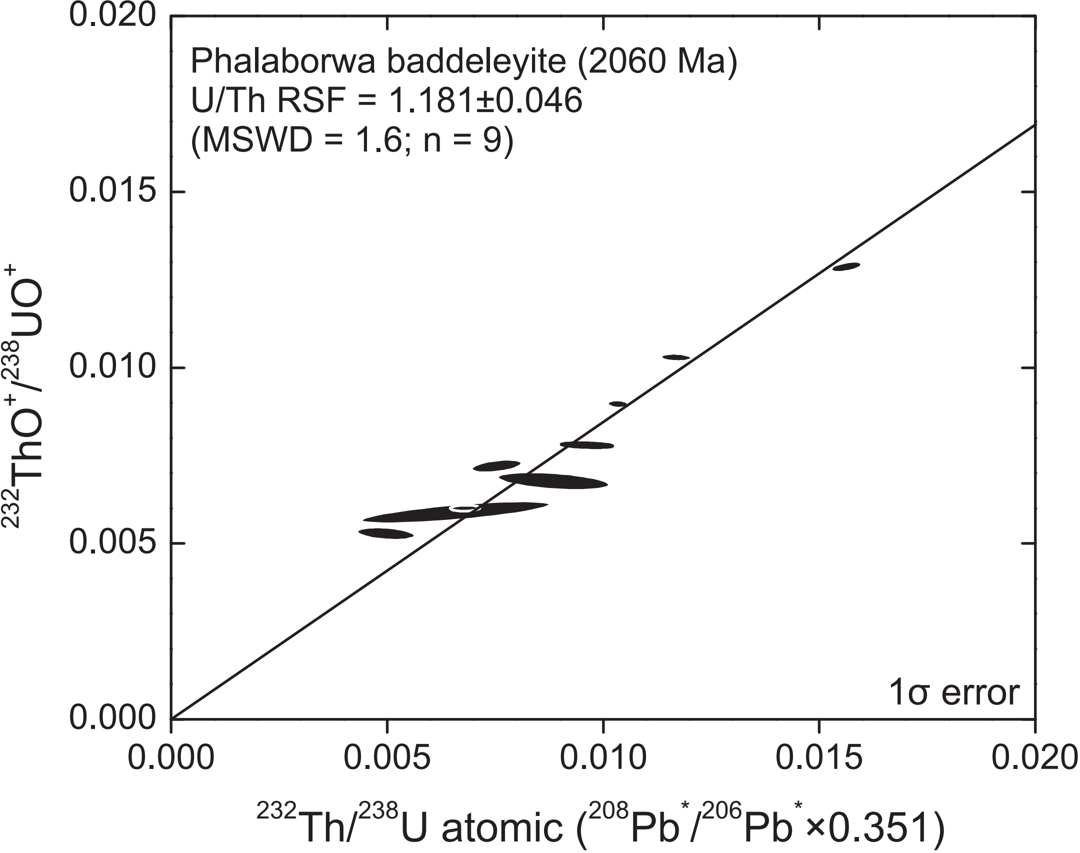

Phalaborwa baddeleyite (2060 Ma)
U/Th RSF = 1.181±0.046
(MSWD = 1.6; n = 9)
1σ error
0.000
0.005
0.010
0.015
0.020
$^{232}ThO^+/^{238}UO^+$
$^{232}Th/^{238}U$ atomic ($^{208}Pb^*/^{206}Pb^*$×0.351)

Fig. 3: Wu et al.

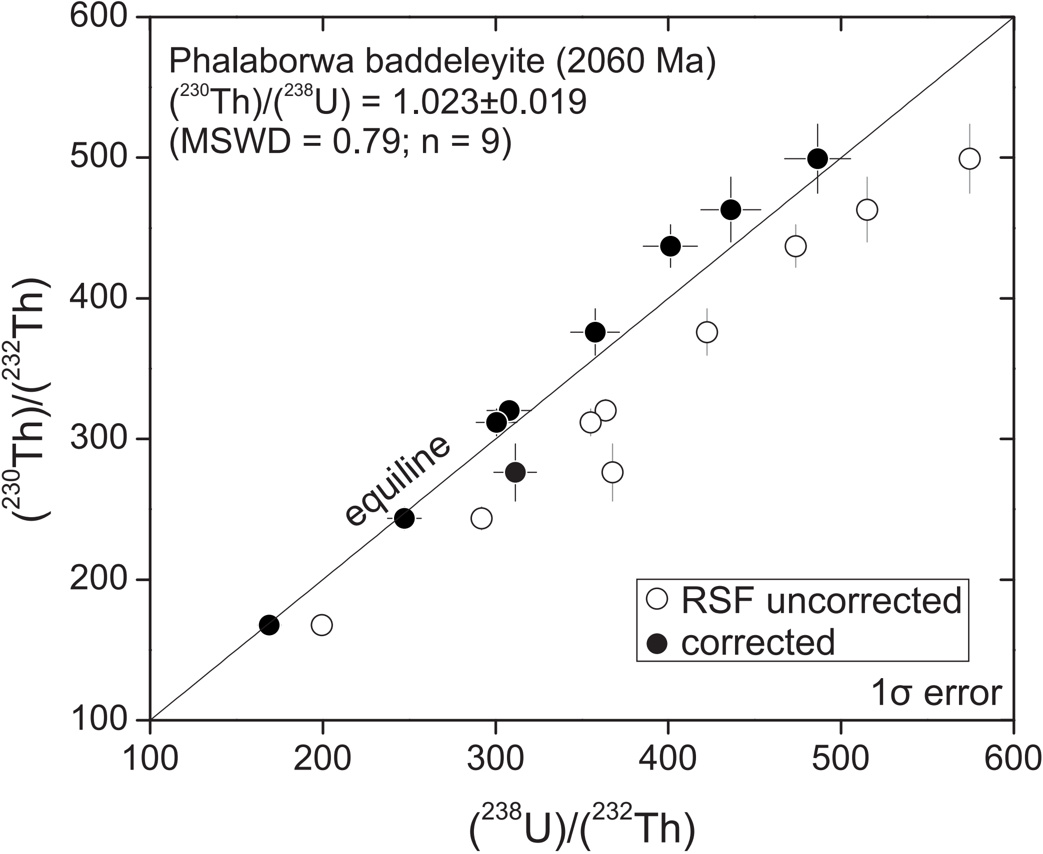

Phalaborwa baddeleyite (2060 Ma)
(230Th)/(238U) = 1.023±0.019
(MSWD = 0.79; n = 9)
equiline
RSF uncorrected
corrected
1σ error
(230Th)/(232Th)
(238U)/(232Th)
100
200
300
400
500
600

Fig. 4: Wu et al.

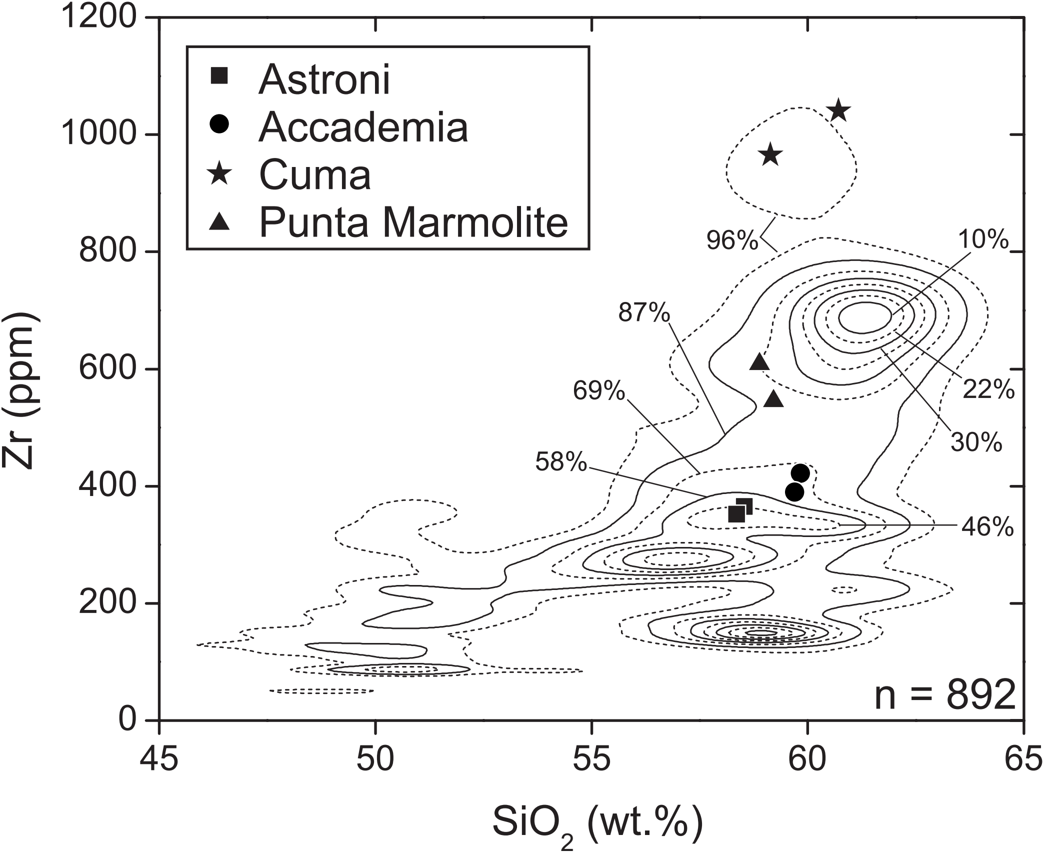
Astroni
Accademia
Cuma
Punta Marmolite
96%
10%
87%
69%
22%
30%
58%
46%
n = 892
1200
1000
800
600
400
200
0
Zr (ppm)
45
50
55
60
65
SiO$_2$ (wt.%)

Fig. 5: Wu et al.

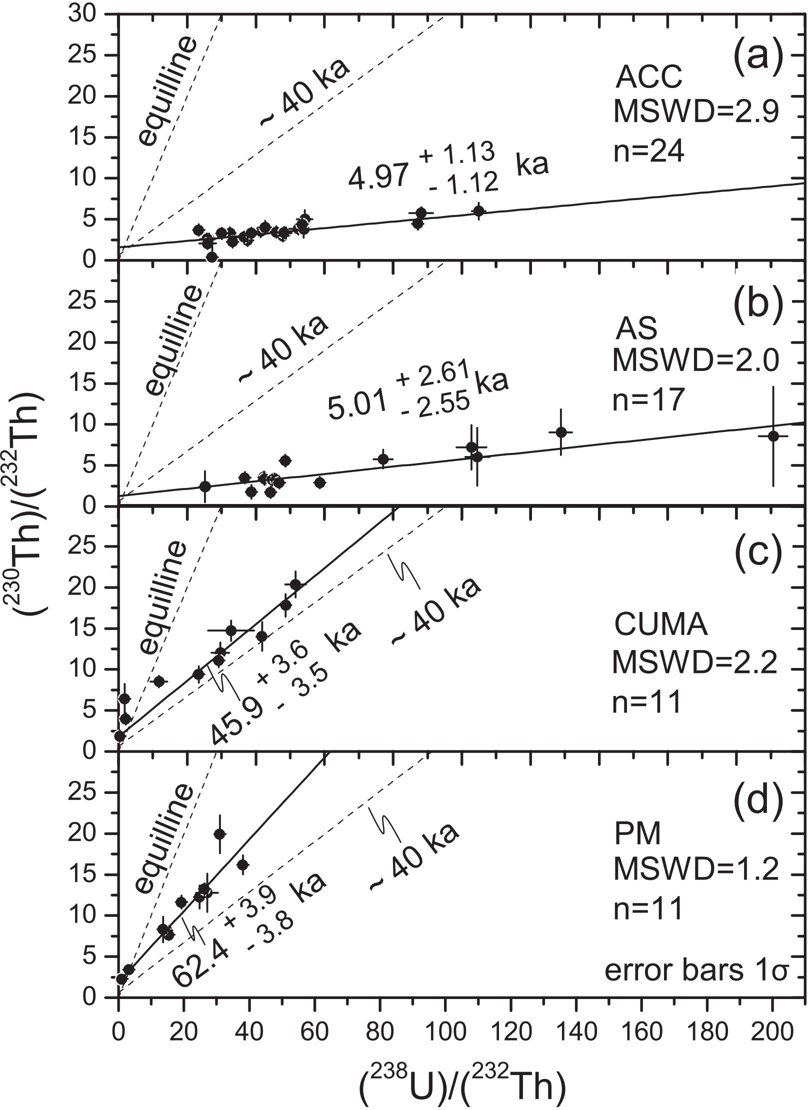

(a)
ACC
MSWD=2.9
n=24
equilline
~ 40 ka
4.97 + 1.13 - 1.12 ka
(b)
AS
MSWD=2.0
n=17
equilline
~ 40 ka
5.01 + 2.61 - 2.55 ka
(c)
CUMA
MSWD=2.2
n=11
equilline
~ 40 ka
45.9 + 3.6 - 3.5 ka
(d)
PM
MSWD=1.2
n=11
equilline
~ 40 ka
62.4 + 3.9 - 3.8 ka
error bars 1σ
(230Th)/(232Th)
(238U)/(232Th)
0
20
40
60
80
100
120
140
160
180
200

Fig. 6: Wu et al.

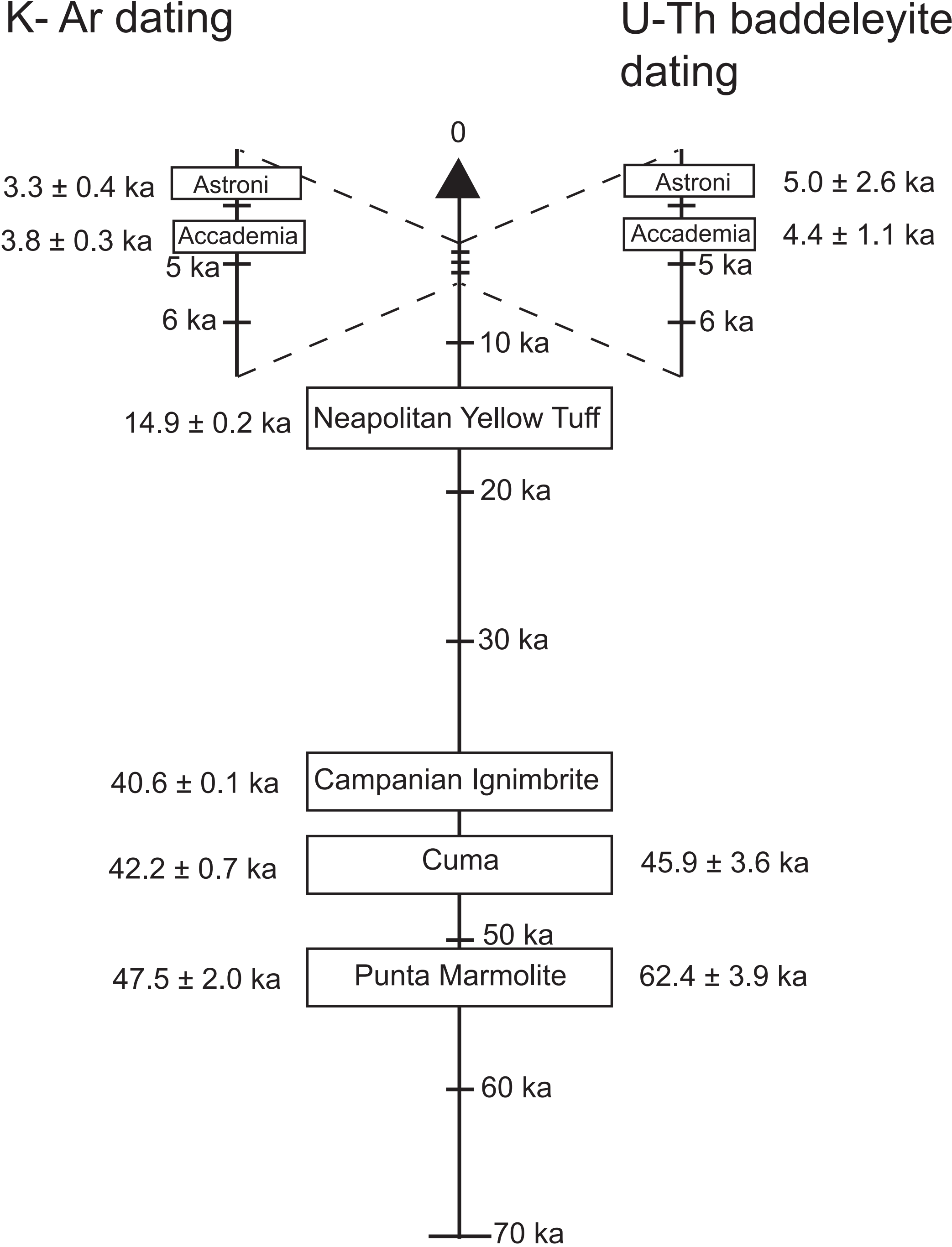
K- Ar dating
U-Th baddeleyite dating
0
3.3 ± 0.4 ka
Astroni
3.8 ± 0.3 ka
Accademia
5 ka
6 ka
10 ka
Astroni
5.0 ± 2.6 ka
Accademia
4.4 ± 1.1 ka
5 ka
6 ka
14.9 ± 0.2 ka
Neapolitan Yellow Tuff
20 ka
30 ka
40.6 ± 0.1 ka
Campanian Ignimbrite
42.2 ± 0.7 ka
Cuma
45.9 ± 3.6 ka
50 ka
47.5 ± 2.0 ka
Punta Marmolite
62.4 ± 3.9 ka
60 ka
70 ka

Fig.7: Wu et al.